Advances in Materials Physics and Chemistry, 2021, 11, 7-19
https://www.scirp.org/journal/ampc
ISSN Online: 2162-5328
ISSN Print: 2162-531X

Experimental Characterization of ALD Grown Al_2O_3 Film for Microelectronic Applications

Yuxi Wang[1,2,3], Yida Chen[4], Yong Zhang[1,2,3], Zhaoxin Zhu[5], Tao Wu[1], Xufeng Kou[1], Pingping Ding[4], Romain Corcolle[4], Jangyong Kim[1,5]

[1]School of Information Science and Technology, ShanghaiTech University, Shanghai, China
[2]Shanghai Institute of Microsystem and Information Technology, Chinese Academy of Sciences, Shanghai, China
[3]University of the Chinese Academy of Sciences, Beijing, China
[4]Division of Engineering and Computer Science, NYU Shanghai, Shanghai, China
[5]ShanghaiTech Quantum Device Laboratory, ShanghaiTech University, Shanghai, China
Email: jangyongkim@shanghaitech.edu.cn

How to cite this paper: Wang, Y., Chen, Y., Zhang, Y., Zhu, Z., Wu, T., Kou, X., Ding, P., Corcolle, R. and Kim, J. (2021) Experimental Characterization of ALD Grown Al_2O_3 Film for Microelectronic Applications. *Advances in Materials Physics and Chemistry*, **11**, 7-19.
https://doi.org/10.4236/ampc.2021.111002

Received: November 17, 2020
Accepted: January 24, 2021
Published: January 27, 2021

Copyright © 2021 by author(s) and Scientific Research Publishing Inc.
This work is licensed under the Creative Commons Attribution International License (CC BY 4.0).
http://creativecommons.org/licenses/by/4.0/
Open Access

Abstract

The study of high dielectric materials has received great attention lately as a key passive component for the application of metal-insulator-metal (MIM) capacitors. In this paper, 50 nm thick Al_2O_3 thin films have been prepared by atomic layer deposition technique on indium tin oxide (ITO) pre-coated glass substrates and titanium nitride (TiN) coated Si substrates with typical MIM capacitor structure. Photolithography and metal lift-off technique were used for processing of the MIM capacitors. Semiconductor Analyzer with probe station was used to perform capacitance-voltage (C-V) characterization with low-medium frequency range. Current-voltage (I-V) characteristics of MIM capacitors were measured on precision source/measurement system. The performance of Al_2O_3 films of MIM capacitors on glass was examined in the voltage range from −5 to 5 V with a frequency range from 10 kHz to 5 MHz. Au/Al_2O_3/ITO/Glass MIM capacitors demonstrate a capacitance density of 1.6 fF/μm^2 at 100 kHz, a loss tangent ~0.005 at 100 kHz and a leakage current of 1.79×10^{-8} A/cm^2 at 1 MV/cm (5 V) at room temperature. Au/Al_2O_3/TiN/Si MIM capacitors demonstrate a capacitance density of 1.5 fF/μm^2 at 100 kHz, a loss tangent ~0.007 at 100 kHz and a lower leakage current of 2.93×10^{-10} A/cm^2 at 1 MV/cm (5 V) at room temperature. The obtained electrical properties could indicate a promising application of MIM Capacitors.

Keywords

Dielectrics, High-*k*, Thin Film Capacitors, Atomic Layer Deposition, Microfabrication

1. Introduction

Following the "More than Moore" paradigm, we have witnessed extensive integration of passive components, *i.e.* capacitors and inductors, for further downscaling of electronics in thin film transistors (TFT), thin film capacitors (TFC) and radio frequency (RF) signal integrated circuit (IC) applications [1]. Among those, metal-insulator-metal (MIM) capacitors have been widely used for their low parasitic capacitance and simple structure [2]. In RF and analog ICs applications, MIM capacitors are required to exhibit desirable electrical characteristics including a high capacitance density, low leakage current, and acceptable voltage linearity [3]. However, most of these works focused on thin film dielectrics, with particular emphasis on SiO_2 (k~3.9), which has a relatively low capacitance density, large leakage current and high interface trap when the width is being minimized in order to increase the capacitance. Various high-k dielectrics to replace SiO_2 have been extensively investigated, such as Si_3N_4, Al_2O_3, HfO_2, TiO_2, La_2O_3 and ZrO_2 for past decades [4]-[9].

Al_2O_3 stands out for its good electrical insulation performance, very large bandgap (E_g ~8.8 eV), desirable thermodynamic stability, excellent chemical stability, high mechanical strength, high temperature resistance (~1600˚C), good biocompatibility [10] and high conduction band offset to semiconductor substrates (Si, SiC, GaN) with relatively low dielectric constant (k~9). Compared to HfO_2, TiO_2 and ZrO_2, Al_2O_3 has a much higher theoretical ultimate breakdown strength E_{bd} at 13.8 MV/cm [11]. Previous work on Al_2O_3 has reported a capacitance density of 1 - 3 fF/μm^2 and a leakage current of 10^{-8} A/cm^2 [12] [13]. To fabricate the ultra-thin high-k dielectric, Atomic Layer Deposition (ALD) is used due to its conformity, control over thickness and composition [3].

Atomic layer deposition (ALD) is a chemical thin film deposition technique based on the sequential use of self-terminating and cyclic gas-surface reactions, where the precursor vapors are dosed over the growth surface one at a time. The cyclic nature of the ALD processes provides excellent control over the film thickness, which is often demanded for today's microelectronic devices with dimensions downscaled to the nanometer level [14]. In addition, the self-limited surface reactions guarantee that the films deposited by ALD grow atomic layer-by-layer which enables a precise control of thickness and a conformal deposition of thin films even on high-aspect-ratio nanostructures. These attractive characteristics have led to the apparent increased industrial interest towards ALD in general, and an explosive growth in the number of scientific publications during the last ten years with ALD technique.

In this work, we focus on the electrical characterization of Al_2O_3 films on glass and Si substrates grown by ALD technique to experimentally understand the electrical properties of thin film capacitors and optimize the growth conditions of Al_2O_3 films for future advanced research works in various applications. We present the dielectric properties of Al_2O_3 films including the influence of DC voltage on their capacitance, loss tangent in low & medium frequency range,

leakage current, structure investigation and surface morphology with different substrates.

2. Sample Preparation

The deposition of Al_2O_3 thin film was performed in a hot-wall ALD system (*Picosun SUNALE™ R200 Advanced*). The indium tin oxide (ITO) pre-coated glass substrates were used as mechanical substrates in order to take advantage of their bulk insulating properties. ITO is known to be a degenerated n-semiconductor and therefore can be treated as a metal [15]. P-type 500 μm thick, one-sided polished Si (100) wafers with a resistivity of 1 - 10 Ω·cm were also used as alternative substrates. After the conventional cleaning of the Si wafers without removing the native oxide with a diluted Hydrofluoric acid (HF) solution, 50 nm-thick TiN was deposited on Si as bottom electrode at 400˚C using $TiCl_4$ and NH_3 plasma gas as the Ti and N sources by Plasma-Enhanced ALD (PEALD). Liquid NH_3 at room temperature was used as the NH_3 plasma source. The plasma power and NH_3 gas flow rate were 2500 W and 150 sccm, respectively. Subsequently these substrates were cleaned using trichloroethylene and acetone within an ultrasonic vibrator and rinsed by isopropanol (IPA). Al_2O_3 were deposited at the same time on ITO pre-coated glass and TiN-coated Si substrates by thermal ALD process using trimethyl-aluminium (TMA) and water vapor (H_2O) as the aluminium and oxygen precursors, respectively. During Al_2O_3 deposition, the ALD chamber was kept with a constant substrate temperature of 250˚C and a background pressure of 200 mTorr during 500 deposition cycles. This resulted in a process dependent Al_2O_3 layer of approximately 50 nm in thickness with the growth rates of 0.01 nm/cycle in agreement with ellipsometric characterization of the film thicknesses (*M-2000, J.A. Woollam Co.*). It was double checked by cross-section Scanning Electron Microscopy (SEM) that no significant variations of deposition rates were observed. ALD recipes for Al_2O_3 are represented in **Table 1**.

For the complete fabrication of the MIM capacitor devices, photolithography and standard lift-off technique were used in order to properly define the array of electrode patterns. Right after Al_2O_3 deposition, film sample was cleaned for 5 minutes in an ultrasonic bath of acetone, then rinsed in IPA and de-ionized (DI) water, and finally dried with nitrogen to remove atmospheric dust and contamination. Photoresist (*Clariant AZ5214E*) was first spin-coated on ITO/Glass and TiN/Si substrates to be 1.4 μm thick and then baked on a hot plate at 100˚C for 1 minute. Photolithography was performed using a Maskless Aligner (*Heidelberg Instruments MLA 150*) system with a dose of 150 mJ/cm^2 and a wavelength

Table 1. Deposition conditions of Al_2O_3 films.

Temperature (˚C)	Growth Rate (nm/cycle)	Carrier Gas (sccm)		Pulse (s)		Purge (s)	
		TMA	H_2O	TMA	H_2O	TMA	H_2O
250	0.1	150	200	0.1	0.1	4	6

of 405 nm. The exposed photoresist was developed in a developer (*Microchemicals AZ 300MIF*) at 25˚C for 50 s and then rinsed with DI water for 30 s to stop the development and clean the sample surface. The samples were blown dry using a steady stream of N_2.

An array of circular top electrode with 150 nm thickness Au was fabricated on Al_2O_3 thin films by electron-beam evaporation (*Explorer Coating System*, *Denton Vacuum*) under high vacuum conditions of 2×10^{-7} Torr. Before Au layer deposition, a 5 nm Cr was deposited as an adhesion layer. Lift-off technique was performed in acetone with ultrasonic agitation for 5 minutes. Sonication was essential for successful lift-off and top gold layers off their original positions into the solvent. Thereafter the sample was rinsed in isopropanol (for about 3 minutes) and DI water, and finally dried with nitrogen to remove the resist and unwanted metal. The diameters of top electrodes are in the range of 200 - 1000 μm in any individual device. The geometry of the layer structure and desired MIM capacitor pattern structure is shown in **Figure 1** with the corresponding thickness for every layer.

3. Measurement

Al_2O_3 thin film was characterized using X-ray diffraction (XRD), to investigate its structural quality, on Empyrean multipurpose X-ray diffractometer (*Malvern Panalytical*) with filtered Cu-K_a radiation source with a wavelength of λ = 1.54056 Å (40 kV, 30 mA). The powder diffraction diagrams were measured from 10˚ to 80˚ in 2θ with 0.04˚ steps and a 20 s counting time. Subsequently, the microstructure of Al_2O_3 thin film was examined by atomic force microscope (AFM) on Dimension Icon (*Veeco Instruments Inc.*) operated in scanning non-contact mode. The physical thickness of Al_2O_3 thin film was measured on Surface Profiler (*Bruker DektakXT*) and was found to be approximately 50 nm. With the top contacts in the form of gold dots (diameter: 200 - 500 μm, thickness: ~150 nm) and plain bottom contacts of ITO and TiN, the capacitance-voltage (C-V) and current density-voltage (J-V) characteristics of MIM capacitors configuration were measured on a Semiconductor Analyzer (*Keysight B1500A*) and on a Precision Source/Measure system (*Keysight B2912A*), respectively. DC bias is applied to the capacitor under test through the microprobe of the probe station (*Cascade Microtech*, 150 *mm Wafer Probe System*) and internal

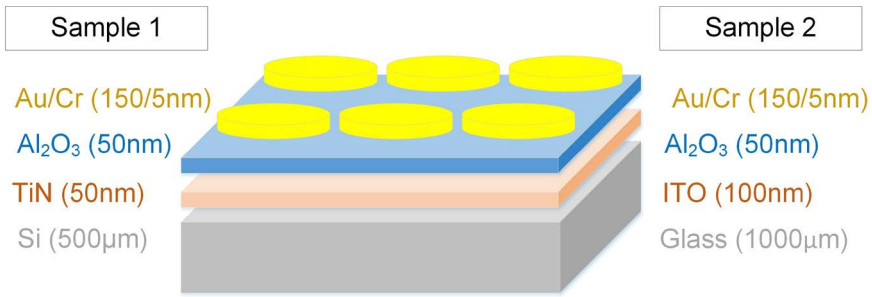

Figure 1. Schematic of MIM Capacitor Au/Al_2O_3/ITO/Glass and Au/ Al_2O_3/TiN/Si.

bias tees of Semiconductor analyzer from −5 V to 5 V. Data were collected at 401 measurement points in the voltage range from −5 V to 5 V with each different frequencies (10 kHz, 100 kHz, 50 kHz, 500 kHz, 1 MHz, 2 MHz, 5 MHz) and were stored in computer files for data analysis. All electrical characteristics were investigated at room temperature without post annealing of MIM capacitors.

4. Results & Discussion

4.1. XRD Characterization

The XRD measurements of the 50 nm thick Al_2O_3 film on ITO/glass and TiN/Si substrates have been performed to evaluate structural and growth quality. Generally, the dielectric properties of high-*k* materials can be affected by the degree of crystallinity, crystal structure, and crystallographic orientation, in addition to their stoichiometric composition. There have been several reports on the dependence of the dielectric constant upon the crystal structure or crystallographic orientation in high-*k* materials [16]. However, crystalized phase can be transformed thermodynamically at high temperature (over 700˚C), whereas the amorphous and monoclinic phase appears at room temperature which is preferable for semiconductor process. Since some studies have been performed to avoid crystallization [17] and control over the amorphous structures is highly demanded, this report strives to understand the dielectric properties of amorphous Al_2O_3 films.

In the XRD θ-2θ scans in **Figure 2** (inset), only single broad diffused reflections can be seen, which confirms that the Al_2O_3 films deposited on ITO/Glass exhibit reasonable amorphous phase. This is also supported by the θ-2θ scans for Al_2O_3 films on TiN/Si substrate which exhibit no additional peaks compared to the scans on TiN/Si substrate alone.

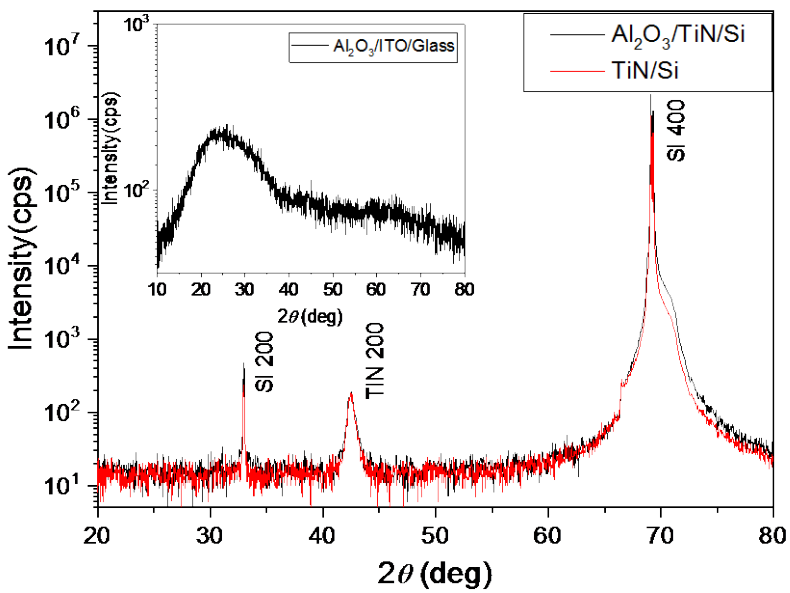

Figure 2. XRD θ-2θ scans for: Al_2O_3 film on TiN/Si substrates and Al_2O_3 film on ITO/Glass substrates (the inset).

4.2. Surface Analysis

Figure 3 shows the AFM height (left) and amplitude (right) images for the Al_2O_3 films deposited on TiN/Si and ITO/Glass substrates. The root-mean-square (RMS) and average surface roughness (R_a) values are shown for indicating the surface morphology.

Thanks to the advantage of ALD technique, a large area uniformity was obtained and, the 250˚C deposited Al_2O_3 films on glass substrates are of little roughness with a root-mean-square (RMS) value of 0.37 nm due to a smooth surface roughness of ITO coating. On the other hand, PEALD TiN films on Si substrates have grown with small particles growing and gathering, leading to the surface roughness increasing with the crystallization. Therefore Al_2O_3 films on Si substrates show 2 times higher roughness value (RMS value: 0.85 nm). A similar trend is observed in R_a values. The increase in surface roughness for the bottom layer thin films might infer a structural change and that may influence the electrical properties.

4.3. Electrical Measurements

The performance of 50 nm Al_2O_3 film on ITO pre-coated glass substrates with 200 μm cylinder shape in the frequency range from 10 kHz to 5 MHz is shown in Figure 4 and Figure 5. A DC bias voltage is applied between the top and bottom electrodes and a small AC voltage is superimposed. C-V single sweep from −5 V to 5 V was performed for every frequency point (10 kHz to 5 MHz).

Figure 4 shows the variation of capacitance with applied voltage for Au/Al_2O_3/ITO/Glass MIM capacitors at different frequencies up to 5 MHz. No previous

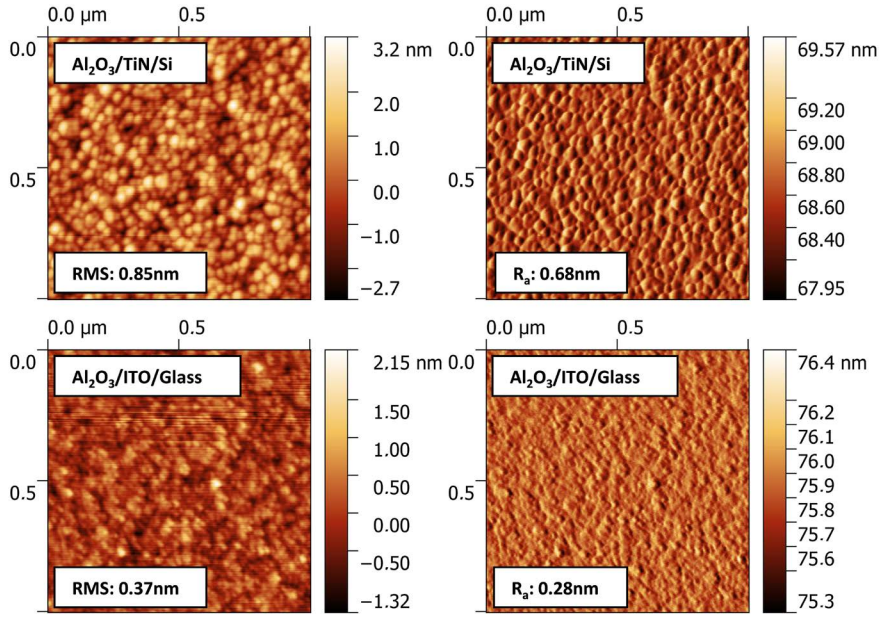

Figure 3. AFM images for: (a), (c) Al_2O_3 film on TiN/Si and ITO/Glass substrates with height trace and (b), (d) Al_2O_3 film on TiN/Si and ITO/Glass substrates with amplitude trace.

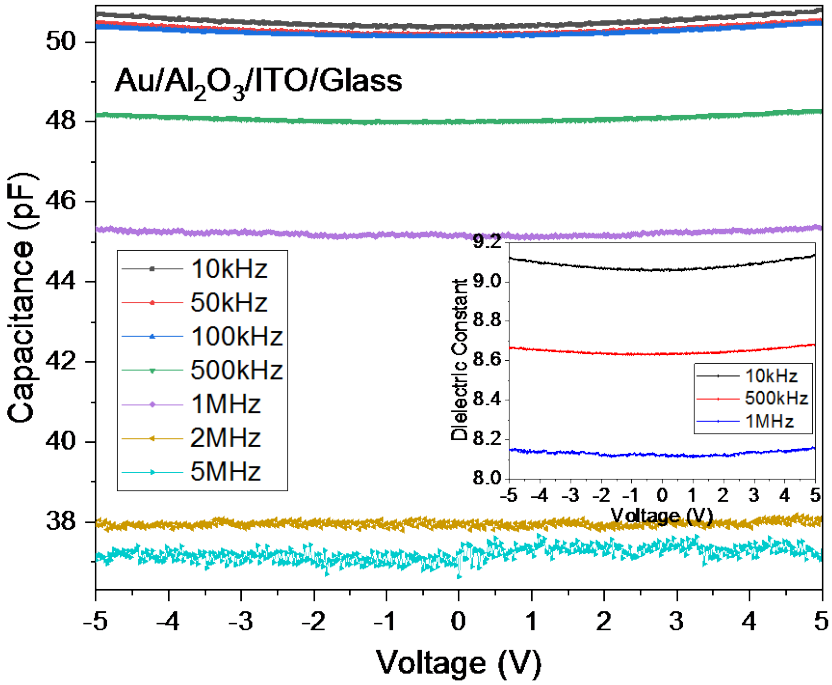

Figure 4. Capacitance and dielectric constant (inset) for Au/Al_2O_3/ITO/Glass MIM capacitor as a function of the DC bias voltage for different frequencies.

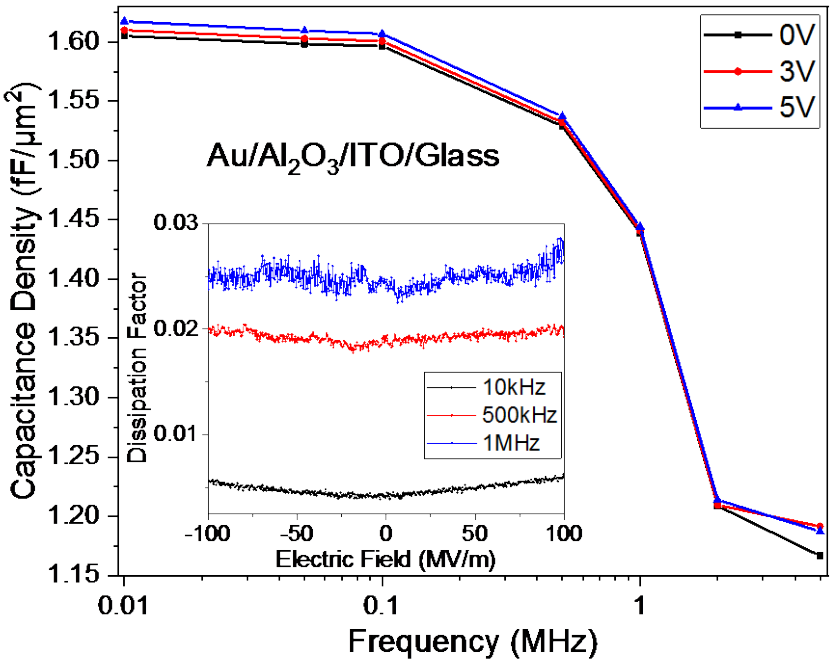

Figure 5. Frequency dependence of capacitance density and dissipation factor (inset) for Au/Al_2O_3/ITO/Glass MIM capacitor with various electric fields at different frequencies.

literature has published experimental C-V data of MIM capacitors over 1 MHz [3] [6]. It is observed that the capacitance remains nearly constant at a fixed applied frequency, which indicates the capacitor's stability under a continuously increasing DC voltage stress. By employing the relationship between the capa-

citance and dielectric constant $C = \varepsilon_0\varepsilon_r (A/d)$, where the ε_0 is the vacuum permittivity ($\varepsilon_0 \sim 8.854 \times 10^{-12}$ F/m), A is the area of device pattern, and d is the thickness of the film, the calculated relative dielectric constant (ε_r) is obtained. It is found that the relative dielectric constant (ε_r) is around 8.15 - 9.15 at 10 kHz - 1 MHz which is in very good agreement with ceramic oxides properties (86% to 99.9% alumina, ε_r = 8.5 - 10.1 at 1 kHz - 1 MHz) [18]. Based on frequency dependent dielectric relaxation, capacitance value decreased from 51 pF to 37 pF as the frequency increases up to 5 MHz. In the range from 10 kHz to 5 MHz, the frequency dispersion of capacitance and dielectric constant were about 26%.

Further, the C-V characteristics can be evaluated using the capacitance densities and dissipation factor shown in **Figure 5**. It can be found that the capacitance densities are 1.2 - 1.6 fF/μm^2 at 10 kHz - 5 MHz when the applied electric field varied from −100 to 100 MV/m which is close to another value (1.55 fF/μm^2) found in literature [19], indicating excellent dielectric characteristics with regard to frequency. The dielectric losses (dissipation factor) appear to increase linearly with the frequency from 0.005 to 0.03 in the frequency range 10 kHz - 1 MHz. Such a low loss factor, with flat dispersion and high capacitance density could demonstrate a reliable integrated MIM capacitor in semiconductor technology depending on the specific electrical characteristics requirements and application.

Figure 6 shows similar results about capacitance and dielectric loss for Au/Al_2O_3/TiN/Si MIM capacitors. The calculated relative dielectric constant (ε_r) is 7.9 - 8.6 at 10 kHz - 1 MHz and capacitance value decreased from 48 pF to 39 pF

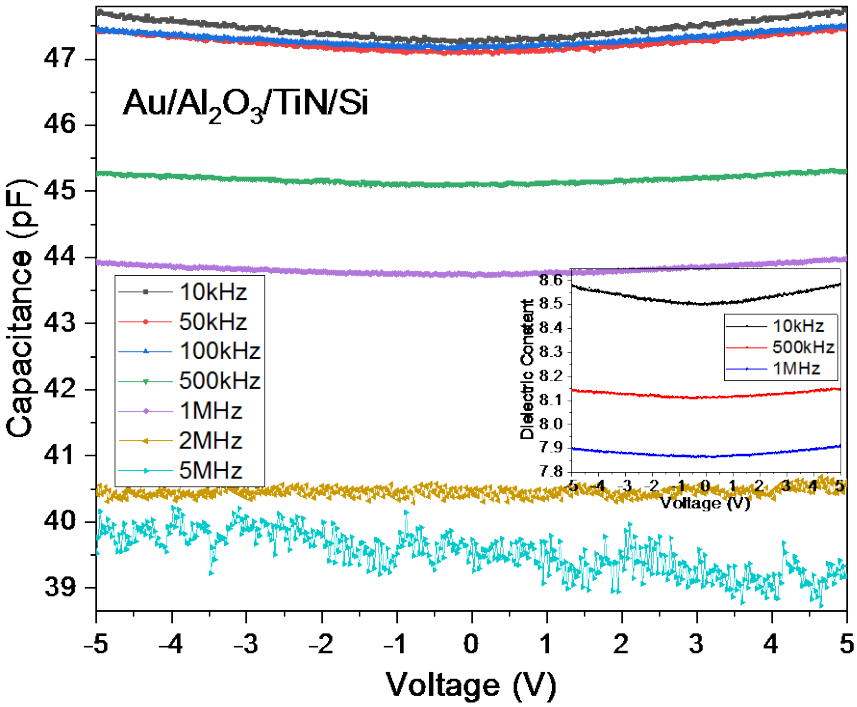

Figure 6. Capacitance and dielectric constant (inset) for Au/Al_2O_3/TiN/Si MIM capacitor as a function of various DC bias voltages for different frequencies.

as the frequency increases up to 5 MHz which is a little lower compared to the values obtained for Au/Al_2O_3/ITO/Glass samples. In the frequency range from 10 kHz to 5 MHz, the frequency dispersion of capacitance and dielectric constant was about 19%. It is attributed to the increasing surface roughness which may result in an electric field stress with the generation of traps in dielectric films and a lower capacitance value [20]. The rougher surface will also affect decreasing capacitance characteristics, which tends to indicate that dielectric loss drastically increased [21]. **Figure 7** shows the capacitance densities (varying from 1.2 to 1.5 fF/μm^2) at 10 kHz - 5 MHz with an applied DC field from −100 to 100 MV/m and the dissipation factor (varying from 0.007 to 0.16) at 10 kHz - 1 MHz. These results seem to confirm that the roughness is one of the major property to optimize in order to improve the quality of the dielectric materials.

Leakage current density is also a crucial parameter for MIM capacitors, particularly at higher voltages. Since the standard thickness of dielectrics is 40 - 50 nm for MIM applications, the quantum phenomenon, where mobile charge carriers (electrons or holes) can tunnel through an insulating material creating conduction paths in it, does not occur. Therefore, conduction only becomes possible because of the activation from electrons or holes. As shown in **Figure 8**, different forward and reverse I-V characteristics are observed due to the different values of the surface roughness at the bottom electrode interfaces which were affected by the Al_2O_3 deposition conditions.

For Au/Al_2O_3/ITO/Glass samples, the sharp increases of forward leakage current (bottom electrode injection) occur at slightly less than 5 V, while for reverse characteristics (top electrode injection) the turning point of the leakage current

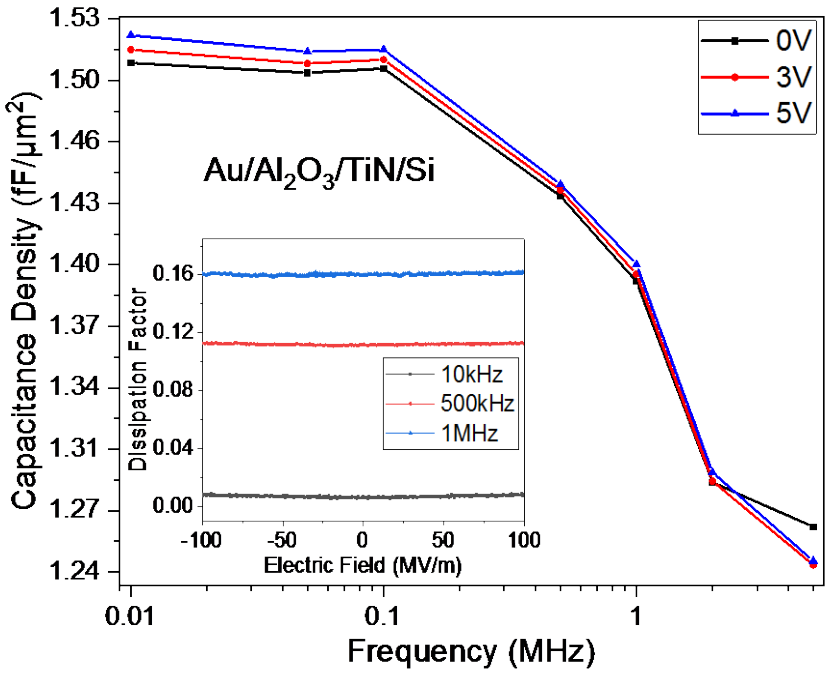

Figure 7. Frequency dependence of capacitance density and dissipation factor (inset) for Au/Al_2O_3/TiN/Si MIM capacitor with various electric fields at different frequencies.

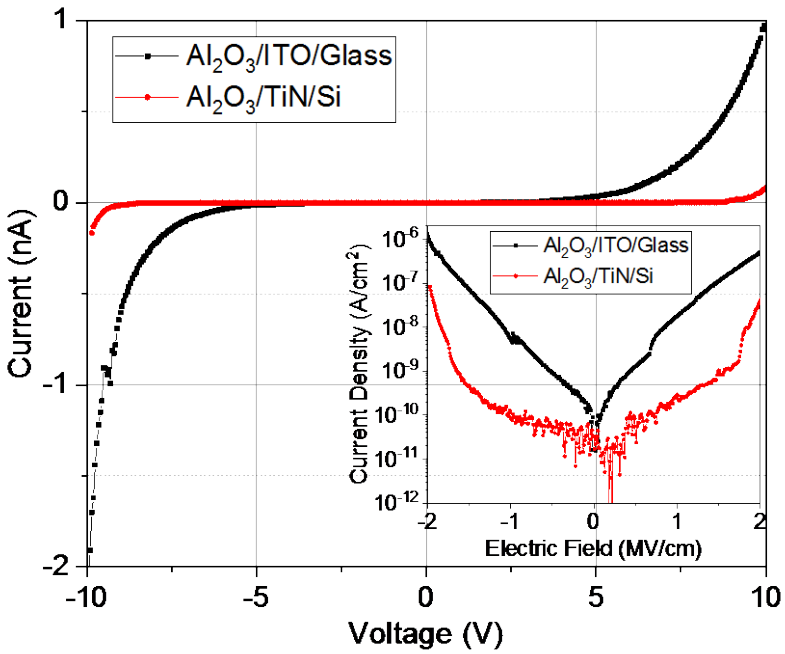

Figure 8. Leakage current and current density (inset) depending on applied DC bias voltages for Al_2O_3 thin films MIM capacitors with different substrates.

occurs at little over −5 V. This represents that the work function of ITO at the bottom interface is smaller than that at the top Al_2O_3/Au interface. Therefore, the electron injection efficiency at the bottom electrode will be larger than the one from the top electrode, irrespective of the type of current conduction. The leakage current density is around 1.79×10^{-8} A/cm^2 at 1 MV/cm (5 V). Au/Al_2O_3/TiN/Si samples show a similar trend and the leakage current density is around 2.93×10^{-10} A/cm^2 at 1 MV/cm (5 V) in room temperature which indicates, to the best of our knowledge, superior data as a single dielectric layer compared with other composites or laminated materials. However, complementary studies of electrical characteristics are necessary to correlate fundamental interface properties with real device behavior.

5. Summary

Aluminum oxide (Al_2O_3) thin film MIM capacitors have been fabricated by atomic layer deposition technique onto ITO pre-coated glass substrates and TiN deposited Si (100) single crystal substrates. Same amorphous orientation of Al_2O_3 films has been investigated by θ-2θ scans of X-ray diffraction measurement. Surface morphology studies for the Al_2O_3 films deposited on different substrates have been performed by AFM technique to indicate the relationship between dielectric properties and thin film surface roughness, caused by the bottom electrode surface roughness. Dielectric characterizations of Al_2O_3 films have been carried out using semiconductor analyzer with probe station for a DC voltage sweep from −5 V to 5 V and specific frequency points from 10 kHz to 5 MHz. Leakage current characteristics of MIM capacitors have been measured on

a precision source/measurement system. Au/Al_2O_3/ITO/Glass MIM capacitors demonstrate capacitance density of 1.6 fF/μm^2 at 100 kHz, a loss tangent ~0.005 at 100 kHz and a leakage current of 1.79×10^{-8} A/cm^2 at 1 MV/cm (5 V) at room temperature. Au/Al_2O_3/TiN/Si MIM capacitors demonstrate capacitance density of 1.5 fF/μm^2 at 100 kHz, a loss tangent ~0.007 at 100 kHz and leakage current 2.93×10^{-10} A/cm^2 at 1 MV/cm (5 V) at room temperature.

Our results demonstrate sufficiently low leakage and high capacitance of MIM Capacitors and suggest the possible use of these MIM Capacitors in analog/RF signal IC applications which can be attributed to the following three factors. First, minimized parasitic MIM structure using precision calibration results in the expansion of frequency range for capacitance measurement up to 5 MHz, thus effectively showing frequency dependent dielectric relaxation. Second, optimizing growth conditions of Al_2O_3 film by ALD technique showed very similar dielectric properties of films grown on either TiN/Si substrates or ITO/Glass substrates, thereby achieving the formation of substrate independent high quality thin film. Third, owing to smooth interface of MIM structure, I-V analysis indicated relatively low leakage current and low loss of single dielectric layer comparable with laminated or composited dielectrics. Finally this experimental review could be helpful for the researchers to get acquainted with the exciting and challenging field of thin film dielectrics of ALD and could be served as a useful guide for the initiators towards the fifth decade of ALD based high-*k* research works.

Acknowledgements

This work was supported by the National Natural Science Foundation of China (Grant No. 61874073) and Quantum Device Laboratory Project.

Conflicts of Interest

The authors declare no conflicts of interest regarding the publication of this paper.

References

[1] Zhang, G.Q., Graef, M. and van Roosmalen, F. (2006) The Rationale and Paradigm of "More than Moore". 56*th Electronic Components and Technology Conference*, San Diego, 30 May-2 June 2006, 151-157.

[2] Zurcher, P., Alluri, P., Chu, P., Duvallet, A., Happ, C., Henderson, R., *et al.* (2000) Integration of Thin Film MIM Capacitors and Resistors into Copper Metallization Based RF-CMOS and Bi-CMOS Technologies. *International Electron Devices Meeting* 2000, San Francisco, 10-13 December 2000, 153-156. https://doi.org/10.1109/IEDM.2000.904281

[3] Pascual, E.M., Jerónimo, G.M., Vargas, H.U., Torres, R.T. and Reyes, J.M. (2020) MIM Capacitors as Simple Test Vehicles for the DC/AC Characterization of ALD-Al_2O_3 with Auto-Correction of Parasitic Inductance. *Microelectronics Reliability*, **104**, 113516. https://doi.org/10.1016/j.microrel.2019.113516

[4] Yu, X.F., Zhu, C.X., Hu, H., Chin, A., Li, M.F., Cho, B.J., *et al.* (2003) A

High-Density MIM Capacitor (13 fF/μm^2) Using ALD HfO_2 Dielectrics. *IEEE Electron Device Letters*, **24**, 63-65. https://doi.org/10.1109/LED.2002.808159

[5] Lin, S.H., Chiang, K.C., Chin, A. and Yeh, F.S. (2009) High-Density and Low-Leakage-Current MIM Capacitor Using Stacked TiO_2/ZrO_2 Insulators. *IEEE Electron Device Letters*, **30**, 715-717. https://doi.org/10.1109/LED.2009.2022775

[6] Chen, S.B., Lai, C.H., Chin, A., Hsieh, J.C. and Liu, J. (2002) High-Density MIM Capacitors Using Al_2O_3 and $AlTiO_x$ Dielectrics. *IEEE Electron Device Letters*, **23**, 185-187. https://doi.org/10.1109/55.992833

[7] Kwon, C.H., Kim, J.H., Jung, I.S., Shin, H. and Yoon, K.H. (2003) Preparation and Characterization of TiO_2-SiO_2 Nano-Composite Thin Films. *Ceramics International*, **29**, 851-856. https://doi.org/10.1016/S0272-8842(03)00019-1

[8] Jõgi, I., Pärs, M., Aarik, J., Aidla, A., Laan, M., Sundqvist, J., *et al.* (2008) Conformity and Structure of Titanium Oxide Films Grown by Atomic Layer Deposition on Silicon Substrates. *Thin Solid Films*, **516**, 4855-4862. https://doi.org/10.1016/j.tsf.2007.09.008

[9] Rathee, D., Arya, S.K. and Kumar, M. (2013) Preparation and Characterization of TiO_2 and SiO_2 Thin Films. *World Journal of Nano Science and Engineering*, **1**, 84-88. https://doi.org/10.4236/wjnse.2011.13013

[10] Rahmati, M. and Mozafari, M. (2019) Biocompatibility of Alumina-Based Biomaterials—A Review. *Journal of Cellular Physiology*, **234**, 3321-3335. https://doi.org/10.1002/jcp.27292

[11] McPherson, J.W., Kim, J., Shanware, A., Mogul, H. and Rodriguez, J. (2003) Trends in the Ultimate Breakdown Strength of High Dielectric-Constant Materials. *IEEE Transactions on Electron Devices*, **50**, 1771-1778. https://doi.org/10.1109/TED.2003.815141

[12] Zhou, J.H., Chang, H.D., Liu, H.G., Liu, G.M., Xu, W.J., Li, Q., Li, S.M., He, Z.Y. and Li, H.O. (2015) MIM Capacitors with Various Al_2O_3 Thickness for GaAs RFIC Application. *Journal of Semiconductors*, **36**, 054004. https://doi.org/10.1088/1674-4926/36/5/054004

[13] Wilk, G.D., Wallace, R.M. and Anthony, J.M. (2001) High-κ Gate Dielectrics: Current Status and Materials Properties Considerations. *Journal of Applied Physics*, **89**, 5243-5275. https://doi.org/10.1063/1.1361065

[14] International Technology Roadmap for Semiconductors. http://public.itrs.net

[15] Lee, K.H., Jang, H.W., Kim, K.-B., Tak, Y.-H. and Lee, J.-L. (2004) Mechanism for the Increase of Indium-Tin-Oxide Work Function by O_2 Inductively Coupled Plasma Treatment. *Journal of Applied Physics*, **95**, 586. https://doi.org/10.1063/1.1633351

[16] Zhao, X. and Vanderbilt, D. (2002) Phonons and Lattice Dielectric Properties of zirconia. *Physical Review B*, **65**, 075105. https://doi.org/10.1103/PhysRevB.65.075105

[17] Lee, F., Dai, J.Y., Wong, K.H., Chan, H.L.W. and Choy, C.L. (2003) Growth and Characterization of Hf-Aluminate High-*k* Gate Dielectric Ultrathin Films with Equivalent Oxide Thickness Less than 10 Å. *Journal of Applied Physics*, **93**, 3665. https://doi.org/10.1063/1.1554764

[18] A Refractory Ceramic Oxide (2001). https://www.azom.com/article.aspx?ArticleID=52

[19] Yota, J., Shen, H. and Ramanathan, R. (2013) Characterization of Atomic Layer Deposition HfO_2, Al_2O_3, and Plasma Enhanced Chemical Vapor Deposition Si_3N_4 as

Metal-Insulator-Metal Capacitor Dielectric for GaAs HBT Technology. *Journal of Vacuum Science Technology A*, **31**, 01A134. https://doi.org/10.1116/1.4769207

[20] Stathis, J.H. (1999) Percolation Models for Gate Oxide Breakdown. *Journal of Applied Physics*, **86**, 5757. https://doi.org/10.1063/1.371590

[21] Albina, A., Taberna, P.L., Cambronne, J.P., Simon, P., Flahaut, E. and Lebey, T. (2006) Impact of the Surface Roughness on the Electrical Capacitance. *Microelectronics Journal*, **37**, 752-758. https://doi.org/10.1016/j.mejo.2005.10.008